

# Tidal Tales Two: The Effect of Dark Matter Halos on Tidal Tail Morphology and Kinematics

J. Christopher Mihos,<sup>1,2</sup> John Dubinski,<sup>3</sup> and Lars Hernquist,<sup>4,5</sup>

## ABSTRACT

We examine the effect of different dark matter halo potentials on the morphology and kinematics of tidal tails in a merger model of NGC 7252. We find that models of merging galaxies with low halo masses of  $M_h \sim 4 - 8M_{disk+bulge}(M_{db})$  can fit the observed morphology and kinematics of the NGC 7252 tails while galaxies with high mass halos ( $M_h \sim 16 - 32M_{db}$ ) fail in this respect. In high mass models, the deep potential only allows weakly bound disk material (stars or gas) at  $R \gtrsim 5$  disk scale lengths to be ejected in tidal tails which tend to fall back onto the parent galaxies before the final merger. Galaxies with massive, low density halos are somewhat more successful at ejecting tidal debris during mergers, but still have difficulties recreating the thin, gas-rich tails observed in NGC 7252. Our models suggest upper limits for the dark halo masses in the NGC 7252 progenitor galaxies of roughly  $M_h \lesssim 10 M_{db}$ . We note, however, that our calculations have focused on the rather idealized case of the isolated merging of galaxies with distinct dark matter halos; calculations which employ more realistic (“cosmological”) initial conditions are needed to fully explore the use of tidal tails in constraining dark matter in galaxies.

*Subject headings:* cosmology:dark matter – dark matter – galaxies:individual (NGC 7252) – galaxies:interactions – galaxies:kinematics and dynamics – galaxies:structure

---

<sup>1</sup>Hubble Fellow

<sup>2</sup>Department of Physics and Astronomy, The Johns Hopkins University, hos@pha.jhu.edu

<sup>3</sup>Canadian Institute for Theoretical Astrophysics, dubinski@cita.utoronto.ca

<sup>4</sup>Presidential Faculty Fellow

<sup>5</sup>Board of Studies in Astronomy and Astrophysics, University of California, Santa Cruz, lars@ucolick.org

## 1. Introduction

While the existence of dark matter halos around galaxies seems well demonstrated through such diverse kinematic tracers as disk galaxy rotation curves (e.g., Rubin et al. 1982, 1985; Kent 1987), satellite galaxies and globular clusters (Zaritsky et al. 1989; Zaritsky & White 1994; Kochanek 1996), and hot gas around ellipticals (e.g., Forman, Jones, & Tucker 1985), the radial extents and total masses of these halos remains poorly constrained. The rotation curves of spiral galaxies generally probe the mass distribution out to only  $\sim 10$  disk scale lengths, while estimates based on more distant satellites are statistical in nature, and sensitive to selection effects and assumptions about orbital kinematics (see, e.g., Zaritsky & White 1994; Kochanek 1996). Taken together, these lines of argument generally suggest that galaxies with circular velocities similar to the Milky Way have halos with masses  $M_{\text{halo}} \sim 10^{12} M_{\odot}$  and extend beyond  $\sim 100$  kpc.

In an attempt to constrain dark matter halos in an independent manner, Dubinski, Mihos, & Hernquist (1996; hereafter DMH) showed that the morphology of tidal tails produced in galaxy collisions depends sensitively on the potential of the galaxies. The use of tidal debris to probe dark matter halos was originally proposed by Faber & Gallagher (1979), and later emphasized by White (1982) and Negroponte & White (1983), who argued that galaxies with massive dark halos might have difficulty forming long tidals due to their deeper potential wells. Barnes (1988) tested these ideas using self-consistent models and noted a weak anticorrelation between the masses of the dark halos of the colliding galaxies and the amount of material ejected in the tidal tails. However, Barnes used galaxies with relatively low mass halos (halo:disk+bulge mass ratios of 0, 4, and 8:1) and concluded that tidal tails are generically easy to produce. Employing halos much more massive than those used by Barnes, DMH demonstrated that if one considers halos as massive and as extended as some observations suggest, the formation of long tidal tails is sharply curtailed. Given that a number of merging galaxies display long tidal tails (e.g., NGC 4038/39, NGC 7252, the Superantennae), DMH argued that such galaxies must have halo:disk+bulge mass ratios on the order of 10:1 or less.

DMH’s study focussed primarily on the *morphology* of tidal tails produced in various galaxy encounters. However, the kinematics of tidal debris may also provide additional constraints which can be compared directly to observed HI kinematics of merging galaxies (e.g., Hibbard 1994; Hibbard & Yun 1997). The kinematics of tidal debris trace the encounter by following trajectories determined in large part by the orbital energy and interaction geometry. Hibbard & Mihos (1995; hereafter HM) used the morphology and kinematics of the extended tidal tails around NGC 7252 to reconstruct the dynamical history of this merger. Their model constrained the orbital geometry and viewing angle of

the encounter as well as the merging timescale, and predicted future infall rates of material currently populating the tidal tails. However, HM used a single halo:disk+bulge mass ratio of 5.8:1 in their simulations and did not investigate in any detail the sensitivity of their results to the internal structure of the merging galaxies.

In what follows, we consider both the morphology and kinematics of tidal tails formed from collisions of galaxies with various halo properties, to provide additional constraints on the amount of dark mass around galaxies as well as to understanding the long term evolution of the tidal debris. Our first step is to examine the kinematics of tidal tails in general, employing models with extended disks of material to trace the dynamics of the loosely bound material from which tidal tails are drawn. We then reanalyze NGC 7252, comparing the morphology and kinematics of the observed tidal tails to those produced in the models. Finally, we address the robustness of the DMH results by considering models with rotating halos and ones with high mass halos having lower central densities and shallower potentials.

## 2. Models

The galaxies used in our study are the self-consistent disk/bulge/halo models developed by Kuijken & Dubinski (1996). Each galaxy consists of a disk and bulge with disk to bulge mass ratio 2:1, embedded in a dark matter halo. In dimensionless units, the disks have a radial scale length  $R_d = 1$ , circular velocity  $v_c(R_d) = 1.0$ , disk mass  $M_d = 0.82$  and bulge mass  $M_b = 0.42$ . When scaled to the Milky Way, these values correspond to  $R_d = 4$  kpc,  $v_c = 220$  km s<sup>-1</sup>,  $M_d = 4.4 \times 10^{10} M_\odot$ , and  $M_b = 2.3 \times 10^{10} M_\odot$ . Four dark halo models are used (Models A – D), varying in their radial extent and total mass, with halo:disk+bulge mass ratios ranging from 4:1 to 30:1 (see Table 1). The models are chosen to have comparably flat rotation curves within 5 disk scale lengths, and deviate only at larger radius (see Figure 1 of DMH).

In addition to a conventional exponential disk, we include a uniform distribution of test particles at  $R = 5 - 10R_d$ . These particles do not contribute to the potential and trace the kinematics of the loosely bound material at large distances which ends up as tidal debris. Because the surface density of material at  $R > 5R_d$  is small, self-gravity in the tidal tails is negligible to their overall kinematic development<sup>6</sup>, justifying the use of massless test particles for this exercise.

---

<sup>6</sup>However, self-gravity is important to the formation of substructure *within* the tails (e.g., Barnes & Hernquist 1992, 1996)

Since our goal is to compare the model kinematics to the observed HI kinematics of NGC 7252, the choice of orbital geometry for the merging galaxies is largely based on the NGC 7252 model of HM. Disk geometry is defined by the inclination ( $i$ ) of the disk to the orbital plane and the argument of periapse ( $\omega$ ) (see Toomre & Toomre 1972). In the HM model, the disk which gives rise to the northwest tail is oriented at  $(i, \omega) = (-40, 0)$ , while the disk forming the east tail has an orientation of  $(i, \omega) = (70, -40)$ . HM used a perigalactic separation of  $R_p = 2.5R_d$ , but noted a degeneracy between  $R_p$  and halo compactness, in that distant mergers with compact halos merged on similar timescales as close passages with more diffuse halos (see also Barnes 1992, DMH). Accordingly, we use two values  $R_p = 2$  and  $R_p = 4$  to examine this effect. Finally, we use a zero energy orbit for the encounters, starting each simulation with the galaxies separated by approximately twice the radius of the halos.

We also follow up attempts by DMH to generate long tidal tails in galaxies with high mass halos by introducing two new galaxy models. The first is motivated by recent studies which suggest that the halos of luminous spirals may have lower circular velocities than that of the disk (Persic, Salucci & Stel 1996; Navarro, Frenk & White 1996). The halos in models such as these may still be quite massive, but would be much more extended and have a shallower potential. We construct a new galaxy Model E with mass intermediate to Models C and D, but with a shallower potential. The rotational speed in the disk is  $V_c(R_d) = 1.0$  while at large radii ( $R > 30R_d$ ),  $V_c \approx 0.7$  and is flat out to  $100R_d$  (Figure 1). The mass of the disk and bulge are  $M_d = 1.13$ ,  $M_b = 0.5$ , slightly larger than in Models A-D to compensate for the lower halo mass within the disk, ensuring the inner rotation curves (at  $R < 5R_d$ ) are similar to models A – D. The total halo mass in Model E is  $M_h = 32$ , intermediate to Models C and D, and the halo extends to  $R=115$ , or nearly 0.5 Mpc (see Table 1).

The second new model incorporates halo rotation into Model D, accomplished by giving all halo particles the same sign of  $z$  angular momentum. The resulting dimensionless spin parameter is  $\lambda = 0.20$ . Halo rotation has been shown to increase the strength of dynamical friction between a halo and a precessing disk (Nelson & Tremaine 1995). Halo rotation might, therefore, lead to more resonances between the halo and passing companion (much like the resonances in the disk which give rise to tidal tails) which could hasten merging and lead to the development of longer tidal tails than in the Model D mergers with non-rotating halos. The spin of these halos is significantly larger than expected from cosmological arguments, which give  $\lambda = 0.05$  (e.g., Warren et al. 1992), so they represent an extreme of this effect if it is present.

Aside from Model E, a total of 160,000 particles were used to represent each galaxy

(320,000 particles per merger simulation): 40,000 in the exponential disks, 20,000 in the bulges, 60,000 in the halos, and 40,000 in the extended test particle disks. In the Model E galaxies, 80,000 particles were used in the disk and 100,000 in the halos. All models were run using a parallel treecode (Dubinski 1996) on the T3D at the Pittsburgh Supercomputing Center. A leapfrog timestep of  $\Delta t = 0.1$  was used, resulting in energy conservation to better than 2%.

We note that our calculations focus on the merging process in isolated environments – there are no neighboring companions, nor is there any ambient potential well in which the galaxies merge (as would be found in cluster or group environments). As such, these models still represent an idealized version of merging and tidal tail formation, and calculations with more realistic (and complex) merger dynamics will be necessary to fully explore the use of tidal tails as a means to constrain dark matter distributions in galaxies.

### 3. Results

#### 3.1. Kinematics of Tidal Debris

We first examine the global kinematics of the tidal tails produced in the encounters. Unfortunately, choosing the most appropriate time to compare the different models is not straightforward. The overall dynamics of both the encounter and the tails depend on the galaxy halos and so the merging times and the times at which the tails achieve their maximum lengths are quite different in the various runs. Consequently, if the models are compared at the same time following the beginning of each simulation, the systems would be in different dynamical states. For simplicity in making the comparison, we choose to “observe” the models one half-mass rotation period after the galaxies have merged<sup>7</sup> in each calculation, and focus on collisions between galaxy Models A–D with  $R_p = 4$ . The morphological and kinematic trends observed in the closer  $R_p = 2$  mergers are qualitatively similar to those in the  $R_p = 4$  mergers described below.

Figure 2 shows the morphology of the tidal tails formed in each encounter (projected onto the orbital plane), along with the energy, radial velocity, and angular momentum as a function of radius along the tidal tails. The self-gravitating particles which form the inner exponential disk (at  $R_{init} < 5R_d$ ) are shown in black, while the outer, flat distribution of test particles is shown in grey.

---

<sup>7</sup>We define “merged” here to mean the point at which the center of mass kinetic energy of the quarter-most bound particles in the central bulges is zero.

Two cautionary notes are in order when interpreting the outer test particles. First, since they are initially distributed with constant surface density, the number of particles increases as  $r^2$ . As a result, the morphology of the outer tails in Figure 2 is dominated by particles at very large radius. In real galaxies the mass distribution is typically dropping with distance, so that tidal debris may be significantly more limited in extent than shown in Figure 2. Second, while the outer parts of galaxies are usually HI dominated, the test particles in our simulations are collisionless and can pass through the galaxies and/or merger remnant without experiencing shocks and dissipation. For example, material seen leading the tidal tails in Model A, or the “third tail” in Model B, comes from particles which passed through the galaxies shortly after the initial collision; gas would likely not survive on such trajectories (e.g., Hernquist & Barnes 1991; Hernquist & Weil 1992). However, most of the material in the extended tails does not suffer such orbit crossing, indicating that the test particles should do a good job of tracing the overall kinematics of extended tidal debris.

The influence of the dark matter halos on the morphology of the tidal tails formed from the inner material is very similar to that described by DMH. Galaxies with low mass halos produce massive, curving tails. As we consider encounters involving galaxies with increasing halo mass, the tails become straighter and more anemic, until for the highest halo mass explored, the tails have nearly disappeared. However, the outer test particles trace the tidal material to larger distances than do the particles in the exponential disk, and show that the tidal debris can be more complex than suggested by DMH.

In Model A, the tails are quite long, and are comprised of particles from both the inner and outer disk. Indeed, it is perhaps surprising that material from the inner disk extends as far out in the tails as does the outer disk material. The latter broadens the tails, and traces the curvature of the tails to larger distances, but is not more extended. The tails are still mostly expanding, with only debris near the base of the tails falling back inwards. The distribution of energy and angular momentum also shows the inner and outer material are well mixed in radius, and the fact that the binding energy along the tail runs smoothly through zero indicates that the outermost material in the tails will continue to expand as the remnant evolves, even as the inner, bound material falls back.

Examining mergers of galaxies with increasing halo mass, the amount of inner disk material in the tails decreases, and is found mostly at smaller distances with lower binding energy. In Model B, the inner disk material still traces the tails, but unlike Model A, none of these particles are unbound. The situation is even more extreme in Model C, where the tails consist entirely of outer test particles, while the inner disk material has fallen back into the remnant to form shells (cf. Hernquist & Spergel 1992; HM). The outer disk material is still expanding in Model C, but the turnaround radius has slowly marched outwards so

that particles within  $40R_d$  are already falling back towards the remnant. None of the inner or outer disk material is unbound in Model C, although the particles with binding energies close to zero will remain at large distances for many Gyrs.

Finally, in the merger of two Model D galaxies, remnant tidal tails are not found in *either* the inner or outer disk material. Tails are launched shortly after the galaxies first collide, but the particles comprising these features are tightly bound to the galaxies and fall back onto the galaxies before they actually merge, as noted by DMH. Consequently, once the merger is complete, the tidal debris has already been accreted by the remnant, surrounding it in the form of loops and shells.

As indicated by Figure 2, the radial extent of the disks can affect the lengths of the tidal tails, an effect not considered by DMH. The more loosely bound material in the outer disks is readily expelled into the tails. Figure 3 shows the radii in the original disks from which material in the tails was drawn. Low mass mergers extract material from deep within the colliding galaxies, sending it to large distances in the tails. For larger halo masses, the inner disk material is more tightly bound to the host galaxy, and the tails are formed from material initially further out. For Model C, only particles with initial radii larger than  $5 - 6R_d$  contribute to the tails, while in Model D, the extended loops are comprised only of material from radii greater than  $7R_d$ .

The fact that tidal tails are formed from material initially at different locations within the progenitors indicates that the amount of mass (or, alternatively, stellar luminosity) comprising the tails may depend sensitively on the asymptotic structure of the colliding disks. To quantify this finding, we can assign masses to the outer test particles *ex post facto* for various adopted initial mass distributions, and derive the total mass of the ensuing tidal tails. The choice for the initial mass distribution depends on the component of interest: stellar disks follow the exponential density profile continued from the inner disk, while HI disks in galaxies generally follow a flatter profile, with more mass at large radii. To span a range of plausible outcomes, we choose four surface density profiles for setting the masses of the test particles:  $\Sigma = \text{constant}$ ,  $\Sigma \sim r^{-1}$ ,  $\Sigma \sim \exp(-r/2R_d)$ , and  $\Sigma \sim \exp(-r/R_d)$ . The cumulative mass profiles of the tidal debris derived by this procedure are shown in Figure 4.

For an outer disk with constant surface density, the tidal debris is quite massive, even for the Model D mergers. However, this is an extreme limiting case, and probably does not reflect the actual HI profiles of disk galaxies. For mass distributions more typical of extended HI disks, 10–20% of the material ends up in the tidal tails, and, for lower mass halos, much of this material is expelled to great distances from the remnant (and is still expanding outwards). In contrast, for similar mass distributions, the Model D merger has only a few percent of this material in the tidal debris; most of the particles remain at small

distances, tightly bound to the remnant. For a pure exponential disk (comparable to the stellar mass distribution in galaxies), the mass in the tails is  $\sim 15\text{--}20\%$  of the *total* disk mass for Model A mergers,  $\sim 10\%$  for Model B mergers, and  $\sim 5\%$  for Model C mergers. The Model D mergers, with no true tails, contain only a few percent of any exponentially distributed material in their tidal debris.

We can compare these values to the HI and stellar luminosity observed in the tidal debris of NGC 7252. Hibbard et al. (1994) find  $\sim 2 \times 10^9 M_\odot$  of HI in the tidal tails, and a blue luminosity for the tails of  $\sim 3 \times 10^9 L_\odot$ , or  $\sim 7\%$  of the total blue luminosity of the system. These values suggest that NGC 7252 is best described by our Model B encounters – the amount of “starlight” in the Model A mergers is too large for the observed blue luminosity of the tails in NGC 7252, while Models C and D have tails that are too anemic, by comparison.

### 3.2. NGC 7252 Comparison

We now compare the simulations directly to the morphological and kinematic properties of NGC 7252 from Hibbard et al. (1994). For each model, we attempt to find the observing geometry and time which best fit the HI data, although in some cases that “best fit” may not be ideal. Our goals are to estimate how unique a given solution is, once variations in halo properties are taken into account, and to see if additional constraints can be placed on the halo properties of the galaxies which collided to form the NGC 7252 system.

We begin by eliminating models which are obviously discrepant. As noted earlier, the tidal debris in Model D collisions has already fallen back into the remnant by the time galaxies merge; extended tidal tails do not persist in this case. Mergers of Model C galaxies are somewhat more difficult to dismiss. Several arguments, however, make these simulations a poor fit to NGC 7252. The tidal tails in the calculation are comprised of material located initially only outside  $6R_d$ ; with an exponential distribution of starlight, this would put  $\sim 0.5\%$  of the stellar luminosity in the tails, an order of magnitude less than the 7% of NGC 7252 starlight ( $L_B$ ) in NGC 7252 actually detected in the tails (Hibbard et al. 1994; see also §4 below). Furthermore, because the tails drawn from the Model C galaxies come entirely from loosely bound outer disk material, they are highly warped, making it difficult to associate them with the relatively thin tidal features observed in NGC 7252. Finally, the Model C tails possess very little of the large-scale curvature needed to reproduce the structure of the northwestern HI tail in NGC 7252. For these reasons, we also reject the Model C mergers as being good matches to NGC 7252.



We focus now on mergers of Model A and B galaxies, which have halo:disk+bulge mass ratios of 4 and 8, respectively.<sup>8</sup> For each simulation, we examined the remnant at two times: one immediately following the final coalescence of the progenitors and another after the remnant has evolved for a few dynamical times. In comparing the model remnant to the observations, three things, in particular, determined the subjective quality of the fit: the curvature of the northwest tail, the kinematic gradients along the tails, and the straightness of the eastern tail. The latter constraint was the most difficult to match, because of the strong warping of the outer disks. If much of the material in the eastern tail of NGC 7252 came from loosely bound gas, the disk giving rise to the eastern tail must have been more closely aligned to the orbital plane than the  $i = 40^\circ$  value of the HM model.

For brevity, we show each model only at the time when it best matches the HI observations of NGC 7252. The HI data from Hibbard et al. (1994) is shown in Figure 5, in the form of the “clean components” of the VLA data cube (see HM for details). Figure 6 shows the morphology and projected kinematics of the four models, and can be directly compared to Figure 5. The best fit time in each case proved to be near  $t = 120$ , or 70 time units ( $\sim 1$  Gyr) after the galaxies first collided. For the Model A and the  $R_p = 2$  Model B simulations, all of which resulted in mergers soon after first passage, the remnant is more evolved than that for the  $R_p = 4$  Model B calculation, where the remnant is somewhat younger.

Figure 6 clearly shows both the difficulty in obtaining an ideal fit, and the degeneracies which complicate matching the simulations to observations. Nonetheless, some trends are apparent with both  $R_p$  and halo mass which help to constrain the parameters. One important diagnostic is the curvature of the NW tail, and it appears that the simulations here bracket a best fit – the Model A mergers have NW tails which are too curved, while the corresponding tails in the Model B mergers are too straight. The curvature of the tails is also manifested by a hook-shaped feature in the kinematic plots (most noticeable in the  $Y - V_r$  projection). These features were *not* reproduced in the dynamical model of HM, because that model did not include any of the extended outer disk material which makes up the hook. The hook is most noticeable in the Model A mergers, and is less apparent in the Model B mergers, again suggesting that the two models bracket a best fit.

As noted above, it proved very difficult to reproduce the linearity of the eastern tail. This problem was hinted at in the HM model; their tail had a slight southern curvature where it joined to the merger remnant. The present models, which include material at

---

<sup>8</sup>Note that the HM model of NGC 7252 employed galaxies with a halo:disk+bulge mass ratio of 5.8, intermediate to our Models A and B.

much larger initial distances than the HM model, emphasize this problem – to varying degrees, all the models have eastern tails which do not extend radially from the remnant. However, the problem is less severe for the Model A mergers when only the portions of the tails which arise from material inside  $R = 5$  (shown in black in Figure 6) are considered. This material is not so strongly warped out of the disk plane, resulting in a more linear eastern tail. This solution is not applicable to the Model B mergers, where the tidal tails arise almost exclusively from the loosely bound outer disk material.

Taken together, the various models indicate that NGC 7252 is best fit by mergers of progenitors with halo masses in the range of  $M_h \sim 4 - 8 \times M_{db}$ . Unfortunately, this estimate is not tightly constrained. Because the curvature of the tidal tails is determined in large part by the orbit of the merging galaxies, there is a tradeoff between halo mass and perigalacticon making similar solutions possible for different choices of the orbital geometry and structure of the galaxies. For example, Models B2 and B4 show that for the same halo, wider encounters produce tails that are more curved. As a result, it may be difficult to distinguish between close collisions of low mass models and wider collisions involving more massive galaxies. This argument cannot be taken to extremes, however, as very distant encounters would not have had sufficient time to merge before the time set by the dynamical state of the tidal tails. For example, distant Model C mergers would have neither the amount of stellar mass in the tails nor the dynamical age necessary for a satisfactory fit to NGC 7252. But within the stated mass estimate given here, many satisfactory solutions will exist – a single, unique solution is probably unattainable.

### 3.3. Variant Halo Models

The Model C and D collisions presented here and in DMH consistently demonstrate the difficulty in producing long stellar tidal tails from merging galaxies with massive halos. However, it is slightly misleading to refer to the halo mass as the only parameter which controls these differences, since it is really the shape and gradient of the galactic potential which determines the evolution. One could add mass to a halo with a shallow potential simply by extending the halo to a greater distance and reducing the central density.

To examine the evolution of tidal tails in mergers of galaxies with massive, low density halos, we set up a collision between two Model E galaxies with zero energy orbits and pericentric distances of  $R_p = 2.0$  and  $4.0R_d$ . Figure 7 shows the evolution of the Model E  $R_p = 4.0$  collision. At first encounter, material is ejected into tidal features, but like the Model C and D galaxies the debris is limited in extent, and largely formed from material beyond  $\sim 5R_d$ . Because of the lowered halo density, dynamical friction is weaker than in the

fiducial mergers, and the merging timescale is very long: 260 time units, or  $\sim 4.5$  Gyr. As a result, the initially-ejected material has ample time to fall back into the galaxies well before they merge. Upon the second passage preceding the merger, this material is re-ejected as the diffuse tidal tails visible in the final remnant.

At first glance, the final stage of the Model E merger looks similar to the low mass mergers (Models A and B), in the sense that it does display extended tidal tails. In detail, however, several problems remain. At intermediate stages, the tidal debris remains wrapped around the galaxies, unlike the long tidal features shown by galaxy pairs such as NGC 4676 (The Mice) or Arp 295 (see, e.g., Hibbard 1995). Once the galaxies have merged, the extended debris is very diffuse, unlike the thin stellar tails of NGC 7252. Furthermore, the tidal tail in the model E merger is made exclusively from material in the outer disk of (collisionless) test particles, which are initially ejected during the first passage, fall back into the galaxy, and are re-ejected during the final merging. Were this material gas-rich, it would likely not follow this collisionless evolution, but instead suffer significant orbit crossing and strong dissipation, making the formation of long tidal tails during the final merging very difficult. Because the extended tidal tails observed in NGC 7252 are very gas-rich, it seems difficult to describe NGC 7252 by a merger of Model E progenitors.

Another alternative model for the halo is one which includes rotation. Rotating dark halos can potentially increase the dynamical braking during a galaxy collision through a stronger resonant coupling between the orbits of the galaxies and the particles making up the halos. This effect is seen in simulations of satellite accretion where satellites quickly sink to the center of a galaxy once they settle into the equatorial plane of the disk, e.g. Quinn, Hernquist & Fullagar (1993), Walker, Mihos & Hernquist (1996). Nelson & Tremaine (1995) have also shown that rotating halos can change the strength and sign of dynamical friction in the context of tilted disks precessing in flattened halos, although their analysis applies equally to any external perturbations. With this motivation, we examined a collision between two Model C galaxies with rotating halos and compared it to the nonrotating halo cases above.

A comparison of the trajectories of the colliding galaxies with and without halo rotation exhibit few significant differences. After their encounter, the galaxies in the two simulations were separated by nearly the same distances and merged at virtually the same time, suggesting that halo rotation in this case has little effect on merging. Not surprisingly, the resulting tidal debris is essentially unchanged from that in the non-rotating model C mergers. Our study is, however, not exhaustive, so it is still possible that halo rotation could have an effect for different galaxy orientations and orbital geometries (perhaps in nearly coplanar, direct encounters), but it had little effect on the evolution of the system

thought to have produced NGC 7252.

Finally, we note that several recent studies suggest that dark matter halos may be significantly non-spherical. Dark matter halos which form in cosmological N-body simulations are strongly triaxial, with minor-to-major axis ratios of  $\sim 1:2$  (e.g., Dubinski & Carlberg 1991; Warren et al. 1992; Steinmetz & Muller 1995). Observations of polar ring galaxies (Sackett et al. 1994) and warped gas disks (Olling 1996) hint at even flatter shapes for dark matter halos. Although still subject to great uncertainties, these results raise the question of how dependant our results are on the assumption of spherical halos. To answer this, we emphasize that the structure of the tidal tails at the time of merging is governed by two factors: (1) the gradient in the potential well, and (2) the merging timescale. The timescale for merging is set largely by the total mass, which determines the encounter velocity irrespective of the halo shape. While the potential gradient is more sensitive to the halo shape, we point out that isopotential contours are significantly rounder than isodensity contours; to make any significant impact on our results, halos must be *extremely* flattened (i.e. disk-like). The usual kinematic disk instabilities (e.g., Ostriker & Peebles 1973) make such “disky” dark matter models highly untenable.

#### 4. Summary and Discussion

The models presented here expand on the work of DMH and HM in two respects. First, we have followed the evolution of material initially located at very large distances in the progenitor galaxies, allowing us to examine the detailed kinematics and morphology of this loosely bound material. In simulations involving mergers of galaxies with increasing halo mass, the tidal debris is drawn primarily from particles located at increasingly large radii within the progenitors, and more of this material remains bound to the merger remnant. The tidal tails which form immediately in mergers involving very massive halos quickly fall back into the galaxies, so that they are no longer visible by the time the galaxies merge. These models reinforce the claim of DMH that observed merger remnants with long tidal tails must have formed from progenitors with relatively small halo:disk+bulge mass ratios. Second, we have explored a variety of halo models in an attempt to reproduce the observed tidal tail morphology and kinematics of NGC 7252, placing some constraints on the dark matter distribution around merging galaxies. Again, the observations are best fit using mergers of galaxies with halo:disk+bulge mass ratios in the range of 4–8. However, we find that precise estimates are difficult because of degeneracies in the solution, as originally suggested by HM.

The tendency of tail material to be drawn from larger initial radii with increasing

halo mass (Figure 3) has implications for recent QSO absorption line studies. Because of abundance gradients in galactic disks, the ability of galaxy interactions to expel metal-rich material to large distances will be sensitive to the mass distributions of dark matter halos. Accordingly, the metallicity of tidal tails may be used as another constraint on the masses of galaxy halos. Absorption lines produced by tidal debris from intervening galaxies have been identified in several QSO spectra (e.g., Sargent & Steidel 1990; Norman et al. 1996); while metallicity estimates are uncertain, if such systems prove to be reasonably metal-rich, it would support the idea that galaxy halos may be less massive than other observational estimates. This argument is similar to the suggestion that low-mass galaxies are more able to eject metal-rich material into the IGM through starburst-driven superwinds (e.g., Heckman, Armus, & Miley 1990); in this case, however, the energy involved in expelling metal-rich material comes from tidal encounters rather than starburst winds.

With the extended disk models showing that galaxies with more massive halos may eject significant amounts of extended HI into tidal tails, the possibility arises that subsequent star formation could convert this gas into stars and produce the long *optical* tidal tails observed in some merger remnants. However, to match observed tidal tails, which contain as much as 10–20% of the blue luminosity of merging galaxies, this star formation must be prodigious. For example, if the optical light in the tidal tails of NGC 7252 were to come from stars formed *in situ*, then  $\sim 80\%$  of the gas in the tails must have been converted into young stars at several  $M_{\odot} \text{ yr}^{-1}$  to reproduce the total blue luminosity and observed (remaining) gas content of the tails. While some star formation is observed in tidal tails, it typically occurs in a few star forming clumps rather than being smoothly distributed, and at much lower rates. Furthermore, the observed colors of tidal tails are more representative of material stripped from the inner disks of galaxies, rather than young stellar populations (Schombert et al. 1990).

We have also investigated interactions using galaxies containing halo models with different internal kinematics and mass distributions. Maximally rotating halos ( $\lambda = 0.20$ ) have no discernible effect on the evolution of a Model C merger and so the amounts of rotation inferred in halos from cosmological arguments ( $\lambda = 0.05$ ) are unlikely to be important for determining the evolution of merging galaxies. Mergers of galaxies with high mass, extended halos (Model E) are able to eject more material into tidal debris, due to their shallower potential wells. However, the tidal debris is very diffuse and suffers significant orbit crossing, making it difficult to identify with the gas-rich tidal features in objects like NGC 7252. However, our models have only examined one representation of a low density halo model and a more systematic study of the effects of low density halos is warranted, especially in light of observational (Casertano and van Gorkom 1991; Persic et al. 1996) and theoretical (Navarro et al. 1996) results which suggest that the most

luminous spiral galaxies may have declining rotation curves.

The models described here address many of the loopholes left open by DMH, supporting the conclusion that long tidal tails are a signature of compact, low-mass halos in the progenitors to a merger. Nonetheless, one limitation of the models still remains: their rather idealistic initial conditions – galaxies with individual, distinct dark matter halos merging in the absence of any background potential. Given recent cosmological simulations which show that galaxy halos often merge before their luminous galaxies do (e.g., Katz, Hernquist, & Weinberg 1992), our simulations may be an oversimplified version of galaxy mergers. In fact, dynamical friction against a background dark matter distribution may hasten merging, allowing massive galaxies to merge before their tidal tails have fallen back into the galaxies. The development of tidal tails will also be affected by the interaction between *three* potential wells (two galactic and one background); the structure and kinematics of the resultant tidal features is difficult to assess without detailed modeling. The next consistency check on our results would therefore be to examine mergers in a more “cosmological” setting, in which galaxies merge in a more diffuse “sea” of dark matter.

In principle, the statistics of tidal tails could be used to infer the properties of dark matter halos. In practice, however, this may be difficult to achieve. While long tidal tails suggest low mass halos, the converse may not necessarily be true – the lack of observed tidal tails may have been the result of an unequal mass merger, an unfavorable orbital geometry (i.e. a retrograde merger), unsuitable progenitors (ellipticals or S0’s), or rapid fading in surface brightness due to kinematic evolution of the tails (e.g., Mihos 1995). Furthermore, sample selection would be fraught with bias – as mergers are generally identified through the presence of tidal debris, care would need to be taken to ensure the sample would not be skewed towards low mass systems with obvious tidal tails.

While a statistical constraint on the dark matter content of galaxies using tidal tails may be problematic, the implications for individual systems seem more clear. For merging galaxies such as NGC 7252, the Antennae, and the Superantennae, the presence of long tidal tails is difficult to reconcile with massive dark matter halos, unless perhaps the halos are very extended and diffuse. While most kinematic probes of the mass distribution in galaxies (i.e. rotation curves, satellite kinematics) yield lower limits on halo masses, the results described here suggest some of the first *upper limits* on the dark matter content of galaxies. As such, it is of immediate interest to test these concepts using both numerical simulation and detailed observational studies of the morphology, kinematics, and metallicity of tidal tails. As coherent kinematic tracers at the largest radius, tidal tails may yet unveil the dark matter halos in which galaxies live.

We thank John Hibbard for many lively discussions and for providing the HI data for comparison with the simulations. We also thank the Aspen Center for Physics, where the first version of this paper was drafted. This work was supported in part by the Pittsburgh Supercomputing Center and the NSF under Grant ASC 93–18185 and the Presidential Faculty Fellows Program. JCM is supported by NASA through a Hubble Fellowship grant # HF-01074.01-94A awarded by the Space Telescope Science Institute, which is operated by the Association of University for Research in Astronomy, Inc., for NASA under contract NAS 5-26555.

## REFERENCES

- Barnes, J.E. 1988, *ApJ*, 331, 699
- Barnes, J.E. 1992, *ApJ*, 393, 484
- Barnes, J.E. & Hernquist, L. 1992, *Nature*, 360, 715
- Barnes, J.E. & Hernquist, L. 1996, *ApJ*, 471, 115
- Casertano, S., & van Gorkom, J.H. 1991, *AJ*, 101, 1231
- Dubinski, J. 1996, *New Astronomy*, 1(2), 133
- Dubinski, J., Mihos, J.C., & Hernquist, L. 1996, *ApJ*, 462, 576 (DMH)
- Faber, S.M., & Gallagher, J.S. 1979, *ARA&A*, 29, 409
- Forman, W., Jones, C., & Tucker, W. 1985, *ApJ*, 293, 535
- Heckman, T.M., Armus, L., & Miley, G.K. 1990, *ApJS*, 74, 833
- Hernquist, L. & Barnes, J.E. 1991, *Nature*, 354, 210.
- Hernquist, L. & Spergel, D.N. 1992, *ApJ*, 399, L117.
- Hernquist, L. & Weil, M.L. 1992, *Nature*, 358, 734.
- Hibbard, J.E. 1995, Ph.D. thesis, Columbia University
- Hibbard, J.E., Guhathakurta, P., van Gorkom, J.H., & Schweizer, F. 1994, *AJ*, 107, 67
- Hibbard, J.E., & Mihos, J.C. 1995, *AJ*, 110, 140 (HM)
- Hibbard, J.E., & Yun, M.S., 1997, in preparation
- Katz, N.S., Hernquist, L., & Weinberg, D.H. 1992, *ApJ*, 399, L109
- Kent, S.M. 1987, *AJ*, 83, 816
- Kochanek, C. 1996, *ApJ*, 457, 228

- Kuijken, K., & Dubinski, J. 1995, MNRAS, 277, 1341
- Mihos, J.C. 1995, ApJ, 438, L75
- Navarro, J.F., Frenk, C.S. & White, S.D.M. 1996, ApJ, 462, 563
- Nelson, R.W., & Tremaine, S. 1995, MNRAS, 275, 897
- Negroponte, J., & White, S.D.M. 1983, MNRAS, 205, 1009
- Norman, C.A., Bowen, D.V., Heckman, T., Blades, C., & Danly, L. 1996, ApJ, in press
- Olling, R.P. 1996, AJ, 112, 481
- Ostriker, J.P., & Peebles, P.J.E. 1973, ApJ, 186, 467
- Persic, M., Salucci, P. & Stel, F. 1996, MNRAS, 281, 27
- Quinn, P.J., Hernquist, L. & Fullagar, D.P. 1993, ApJ, 403, 74
- Rubin, V.C., Burstein, D., Ford, W.K., & Thonnard, N. 1985, ApJ, 289, 81
- Rubin, V.C., Ford, W.K., Thonnard, N., & Burstein, D. 1982, ApJ, 261, 439
- Sackett, P.D., Rix, H.-W., Jarvis, B.J., & Freeman, K.C. 1994, ApJ, 436, 629
- Sargent, W.L.W., & Steidel, C.C. 1990, ApJ, 359, L37
- Schombert, J.M., Wallin, J.F., & Struck-Marcell, C. 1990, AJ, 99, 497
- Steinmetz, M., & Muller, E. 1995, MNRAS, 276, 549
- Toomre, A., & Toomre, J. 1972, ApJ, 178, 623
- Walker, I.R., Mihos, J.C. & Hernquist, L. 1996, ApJ, 460, 121
- Warren, M.S., Quinn, P.J, Salmon, J.K., & Zurek, W. 1992, ApJ, 399, 405
- White, S. 1982, in *The Morphology and Dynamics of Galaxies*, ed. L. Martinet & M. Mayor (Sauverny: Geneva Obs.), 289
- Zaritsky, D., & White, S.D.M. 1994, ApJ, 435, 599
- Zaritsky, D., Olszewski, E.W., Schommer, R.A., Peterson, R.C., & Aaronson, M. 1989, ApJ, 345, 759



Table 1: Galaxy Model Properties

Model	$M_d$	$M_b$	$M_h$	$R_{\frac{1}{2}}/R_d$	$R_t/R_d$	$M_h/M_{db}$
	(1)	(2)	(3)	(4)	(5)	(6)
A	0.82	0.42	5.2	3.5	21.8	4
B	0.82	0.42	9.6	6.0	30.1	8
C	0.82	0.42	19.8	9.1	44.0	16
D	0.82	0.42	37.0	13.6	72.8	30
E	1.14	0.50	32.1	30.0	115.5	20

Note. — (1) disk mass, (2) bulge mass, (3) halo mass, (4) half mass radius (5) tidal radius (where density drops to zero) (6) ratio of halo to disk+bulge mass.

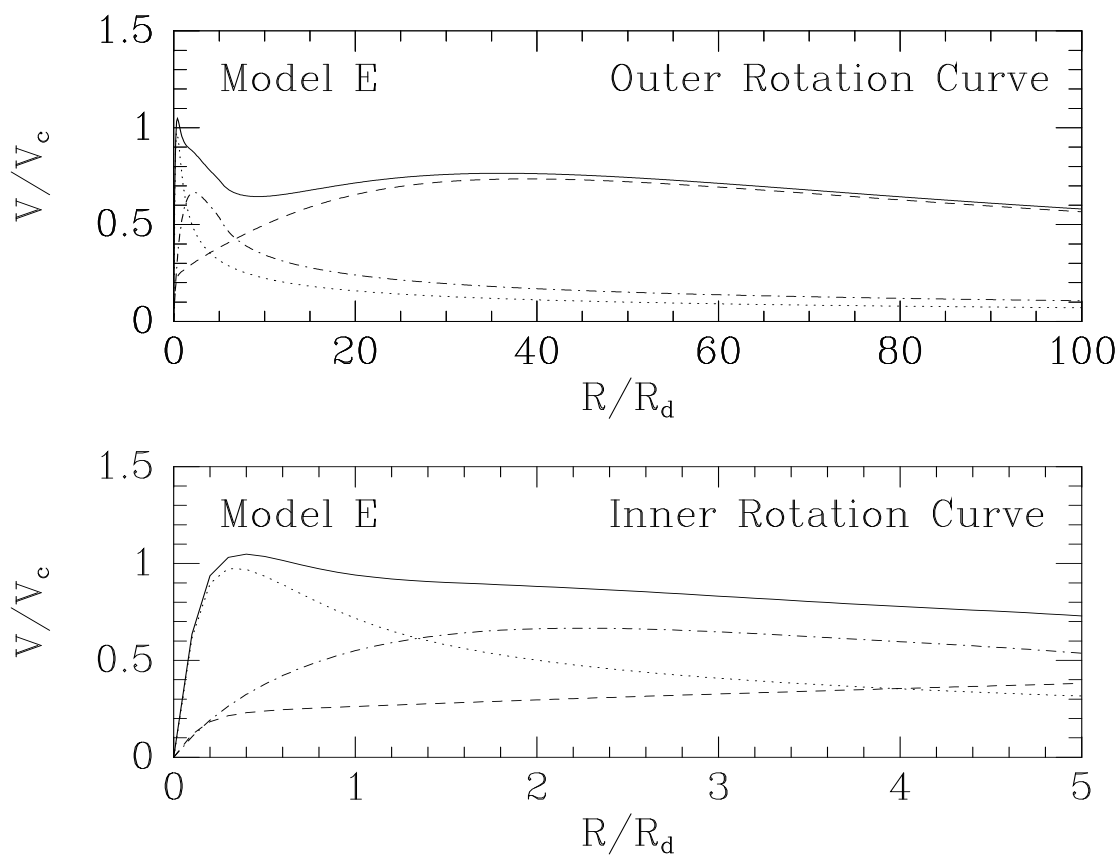


Fig. 1.— Rotation curves of the inner and outer regions of Model E. The total mass of this model intermediate to the high mass models C and D, but the lower central density leads to a more extended, shallower potential. The velocity in the inner region is  $V_c \sim 1.0$  but drops off asymptotically to  $V_c \sim 0.7$  at large radii.

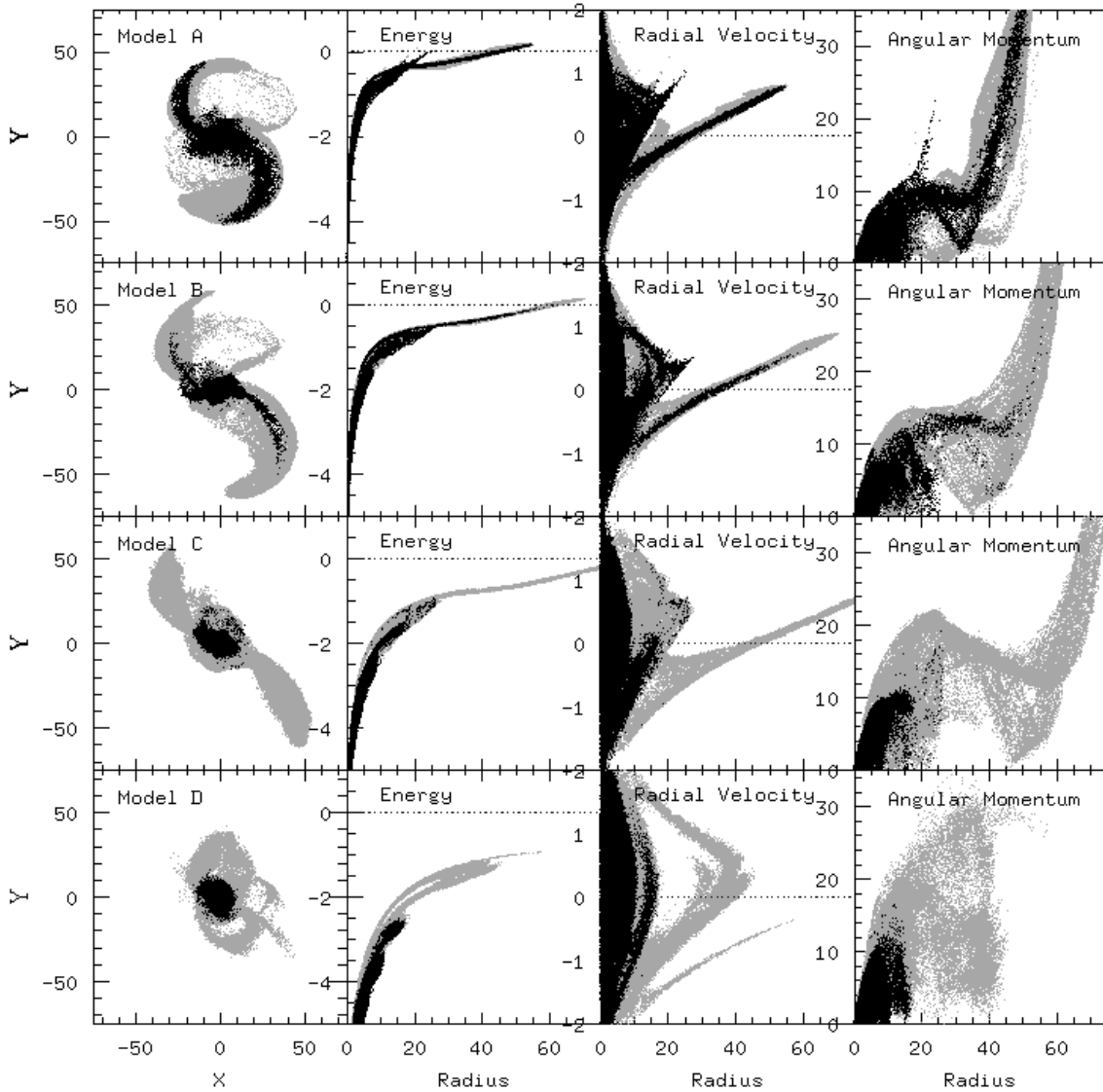


Fig. 2.— Morphology and kinematics of the  $R_p = 4$  merger models, viewed one half-mass rotation period after the galaxies have merged. From left, the panels show the morphology of the tails (projected onto the orbital plane), and the energy, radial velocity (with respect to the central merger remnant), and angular momentum of the tidal material as a function of radius.

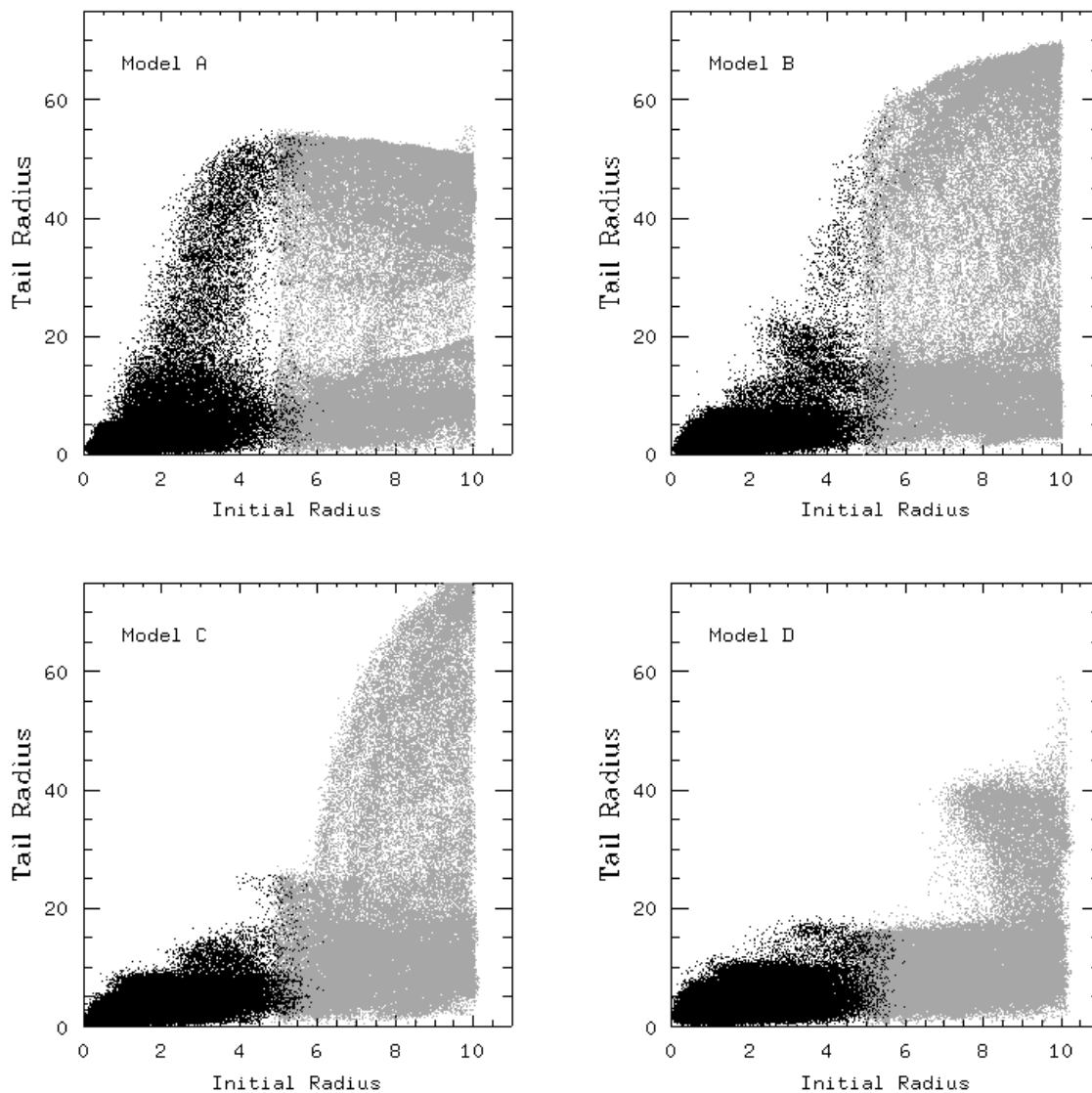


Fig. 3.— Tail radius versus initial radius for the models shown in Figure 2. “Tail radius” is defined as the radial distance of material in the tidal tails one half-mass rotation period after the galaxies have merged. Mergers involving galaxies with low mass halos draw material from deep within the progenitor disks, while the debris formed in mergers of galaxies with massive halos is comprised only of loosely bound material from the extreme outer portions of the disks.

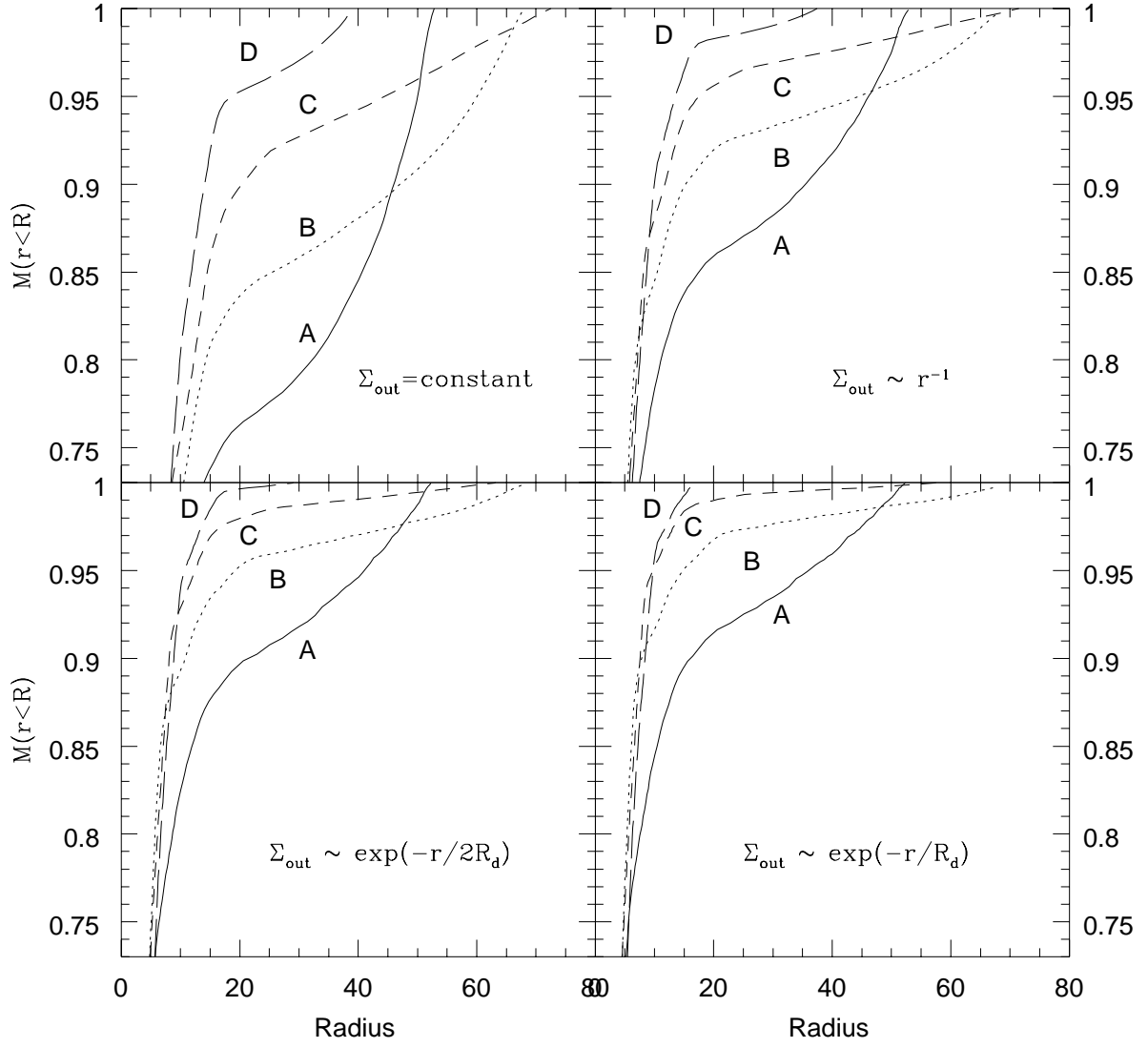


Fig. 4.— Cumulative mass distribution for the mergers shown in Figure 2, under the assumption of varying initial mass distributions for the test particle material at  $R_{\text{init}} > 5R_D$ .

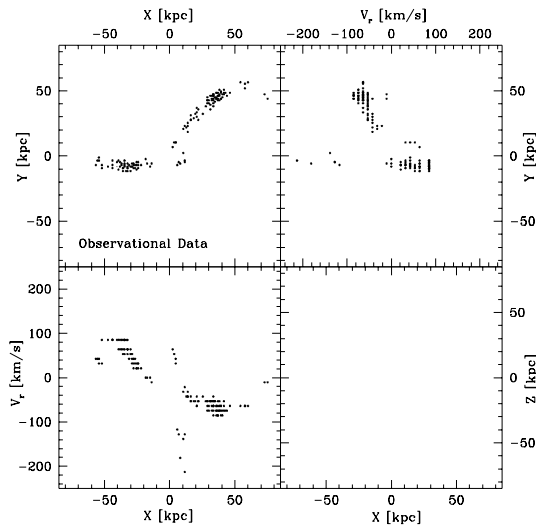


Fig. 5.— HI morphology and kinematics of NGC 7252 (from Hibbard et al. 1994; Hibbard & Mihos 1995). The “clean components” of the HI data cube are shown (see Hibbard & Mihos 1995 for details). The panels show the HI morphology (upper left),  $Y - V_r$  position-velocity diagram (upper right), and  $V_z - X$  position-velocity diagram (lower left).

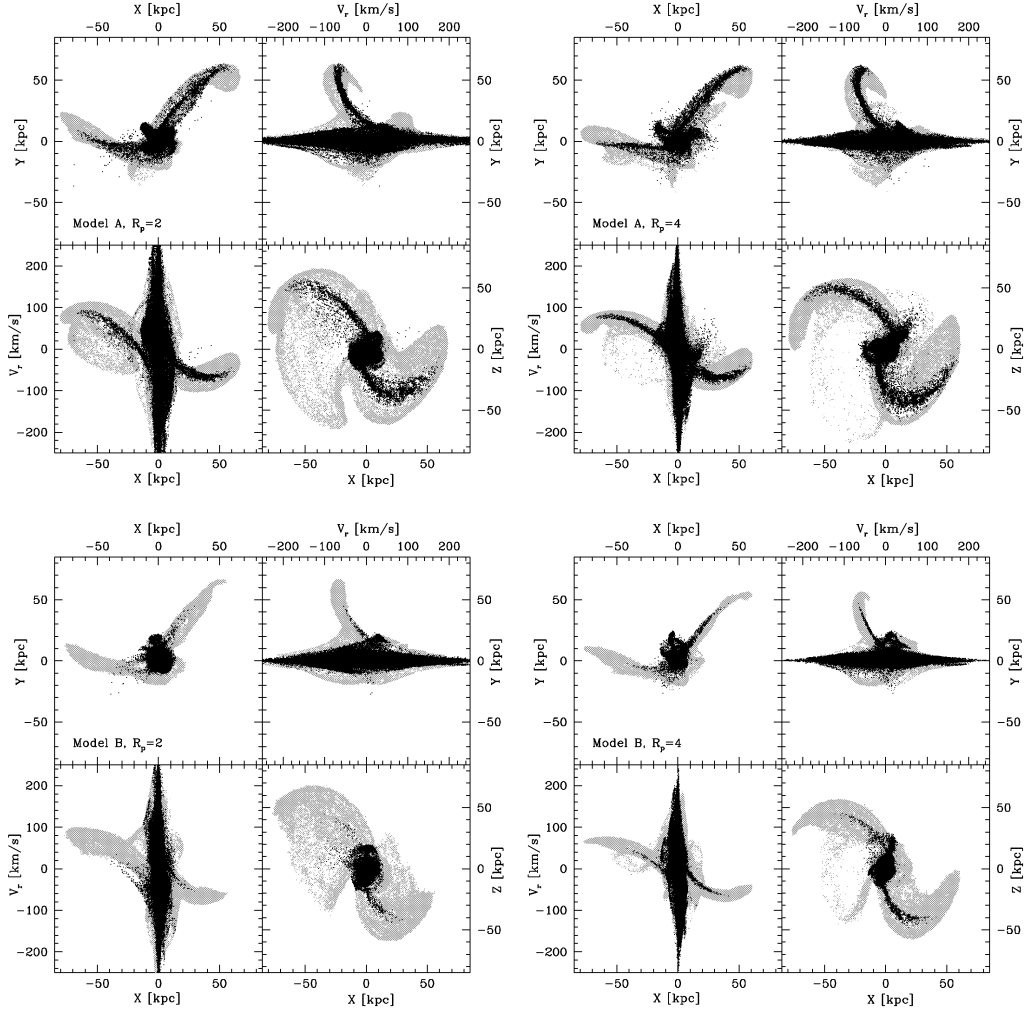


Fig. 6.— Projection of 4  $N$ -body models for comparison with the observed HI morphology and kinematics of NGC 7252 (5). Each subframe compares the morphology (upper left),  $Y - V_r$  position-velocity diagram (upper right), and  $V_z - X$  position-velocity diagram (lower left), and also shows a “top view” of model remnant (lower right).

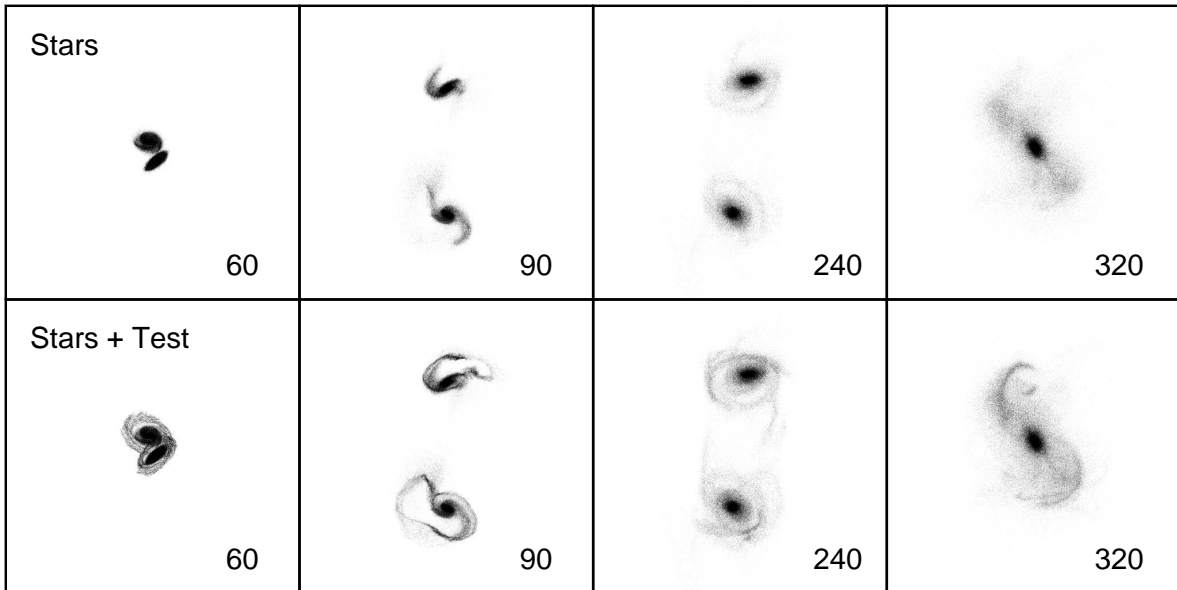


Fig. 7.— Evolution of the Model E interaction with  $R_p = 4.0$  in the orbital plane. Top: Exponential disk particles ( $R < 5R_d$ ) only. Bottom: Exponential disk plus outer test particles. Each box is 100 units wide (400 kpc) and time is shown in each frame (unit time equals 17 Myr). The dynamical breaking is weak in these models because of the smaller central halo density and so the galaxies pass by each other quickly. The short duration of the encounter leads to the modest excitation of some tidal arms which fall back onto the galaxy before the second encounter. Fairly long tidal tails are ejected during the final merger although they are composed of material beyond  $R \gtrsim 5R_d$ .



This figure "fig2.gif" is available in "gif" format from:

<http://arxiv.org/ps/astro-ph/9708009v1>

This figure "fig3.gif" is available in "gif" format from:

<http://arxiv.org/ps/astro-ph/9708009v1>

This figure "fig6.gif" is available in "gif" format from:

<http://arxiv.org/ps/astro-ph/9708009v1>